Magnetic Properties of Rocks and Minerals

Christopher P. Hunt, Bruce M. Moskowitz, Subir K. Banerjee

1. INTRODUCTION

This is an updated collation of magnetic parameters of rocks and minerals for geologists, geochemists, and geophysicists. Since the publication of the previous edition of Handbook of Physical Constants [74], two other collations have appeared [16, 18]. In addition, selected magnetic parameters have also been assembled [19, 22, 38, 41, 88]. Rather than produce a fully comprehensive collection, we have aimed for high-precision data obtained from well-characterized samples.

Both tables and figures have been used for presenting the data, and best-fit equations have been provided for some of the displayed data so that interpolations can be made easily. In an attempt to discourage the use of the outdated cgs system, all values are in the SI system (see Moskowitz, this volume). References have been cited for the sources used here. However, a more comprehensive bibliography has also been provided from which information can be extracted for samples which have not been included.

The single-crystal constants and their variation with temperature and composition are for use by rock magnetists. Paleomagnetists and magnetic anomaly modelers have been provided with the magnetic properties of rocks and polycrystalline mineral samples. Lastly, we have made an effort to address the needs of environmental magnetists, a new group of researchers who require the values of size- and composition-dependent magnetic parameters of a variety of iron-bearing minerals.

C. P. Hunt, B. M. Moskowitz, and S. K. Banerjee, University of Minnesota, Institute for Rock Magnetism and Department of Geology and Geophysics, 310 Pillsbury Drive SE, Minneapolis, MN 55455

Rock Physics and Phase Relations
A Handbook of Physical Constants
AGU Reference Shelf 3

2. MAGNETIC SUSCEPTIBILITY

Magnetic susceptibility is a measure of the magnetic response of a material to an external magnetic field. The volume susceptibility k, measured in dimensionless units, is defined as the ratio of the material magnetization J (per unit volume) to the weak external magnetic field H:

$$J = kH. \tag{1}$$

Alternatively, the specific or mass susceptibility χ, measured in units of m^3kg^{-1}, is defined as the ratio of the material magnetization J (per unit mass) to the weak external magnetic field H:

$$J = \chi H. \tag{2}$$

All materials have magnetic susceptibility, which can be either positive (paramagnetic) or negative (diamagnetic). In materials which display hysteresis, the initial slope of the hysteresis loop is taken to be the initial or low-field susceptibility χ_0. Magnetic susceptibility values are useful in geophysical exploration, and in models of both crustal magnetization and magnetic anomalies. Table 1 lists the (initial) susceptibility for common rocks and minerals.

In ferro-, ferri-, or canted antiferromagnetic materials, hysteresis and the presence of magnetic domains cause the initial susceptibility to become grain-size dependent. This dependence for magnetite is plotted in Figure 1.

Initial magnetic susceptibility is temperature dependent. The susceptibility of paramagnetic materials is inversely proportional to absolute temperature, but the susceptibility

TABLE 1. Magnetic Susceptibilities of Selected Rocks and Minerals

Rock/Mineral	Chemical Formula	Density (10^3 kg m^{-3})	Volume k (10^{-6} SI)	Mass χ (10^{-8} m^{3}kg^{-1})	References
Igneous Rocks					
andesite		2.61	170,000	6,500	114
basalt		2.99	250–180,000	8.4–6,100	95, 107, 114, 115
diabase		2.91	1,000–160,000	35–5,600	114
diorite		2.85	630–130,000	22–4,400	114, 115
gabbro		3.03	1,000–90,000	26–3,000	95, 107, 114, 115
granite		2.64	0–50,000	0–1,900	95, 107, 114, 115
peridotite		3.15	96,000–200,000	3,000–6,200	114
porphyry		2.74	250–210,000	9.2–7,700	114
pyroxenite		3.17	130,000	4,200	114
rhyolite		2.52	250–38,000	10–1,500	114
igneous rocks		2.69	2,700–270,000	100–10,000	22
average acidic igneous rocks		2.61	38–82,000	1.4–3,100	114
average basic igneous rocks		2.79	550–120,000	20–4,400	114
Sedimentary Rocks					
clay		1.70	170–250	10–15	114
coal		1.35	25	1.9	114
dolomite		2.30	-10–940	-1–41	95, 114
limestone		2.11	2–25,000	0.1–1,200	22, 107, 114, 115
red sediments		2.24	10–100	0.5–5	22
sandstone		2.24	0–20,900	0–931	107, 114, 115
shale		2.10	63–18,600	3–886	114
average sedimentary rocks		2.19	0–50,000	0–2,000	114
Metamorphic Rocks					
amphibolite		2.96	750	25	114, 115
gneiss		2.80	0–25,000	0–900	107, 114, 115
granulite		2.63	3,000–30,000	100–1,000	126
phyllite		2.74	1,600	60	114
quartzite		2.60	4,400	170	114
schist		2.64	26–3,000	1–110	114, 115
serpentine		2.78	3,100–18,000	110–630	114
slate		2.79	0–38,000	0–1,400	107, 114, 115
average metamorphic rocks		2.76	0–73,000	0–2,600	114
Non-Iron-Bearing Minerals					
graphite	C	2.16	-80–200	-3.7–-9.3	16, 95, 107, 114
calcite	$CaCO_3$	2.83	-7.5–-39	-0.3–-1.4	16, 18, 22, 114
anhydrite	$CaSO_4$	2.98	-14–60	-0.5–-2.0	16, 18, 95
gypsum	$CaSO_4 \cdot 2H_2O$	2.34	-13–29	-0.5–-1.3	16, 107, 114
ice	H_2O	0.92	-9	-1	107
orthoclase	$KAlSi_3O_8$	2.57	-13–-17	-0.49–-0.67	16
magnesite	$MgCO_3$	3.21	-15	-0.48	22
forsterite	Mg_2SiO_4	3.20	-12	-0.39	16
serpentinite	$Mg_3Si_2O_5(OH)_4$	2.55	3,100–75,000	120–2,900	107
halite	NaCl	2.17	-10–-16	-0.48–-0.75	16, 18, 107, 114
galena	PbS	7.50	-33	-0.44	16
quartz	SiO_2	2.65	-13–-17	-0.5–-0.6	16, 18, 22, 73, 95
cassiterite	SnO_2	6.99	1,100	16	114
celestite	$SrSO_4$	3.96	-16–-18	-0.40–-0.450	16
sphalerite	ZnS	4.00	-31–750	-0.77–19	16, 114

TABLE 1. (continued)

Iron-Bearing Minerals					
garnets	$A_3B_2(SiO_4)_3$	3.90	2,700	69	16
illite	clay w/1.4% FeO, 4.7% Fe_2O_3	2.75	410	15	18, 22
montmorillonite	clay w/ 2.8% FeO, 3.0% Fe_2O_3	2.50	330–350	13–14	18, 22
biotites	$K(Mg,Fe)_3(AlSi_3O_{10})(OH)_2$	3.00	1,500–2,900	52–98	16, 18, 22
siderite	$FeCO_3$	3.96	1,300–11,000	32–270	16, 18, 47, 73, 114
chromite	$FeCr_2O_4$	4.80	3,000–120,000	63–2,500	114
orthoferrosilite	$FeSiO_3$	4.00	3,700	92	18
orthopyroxenes	$(Fe,Mg)SiO_3$	3.59	1,500–1,800	43–50	16, 18, 22
fayalite	Fe_2SiO_4	4.39	5,500	130	18
olivines	$(Fe,Mg)_2SiO_4$	4.32	1,600	36	16
jacobsite	$MnFe_2O_4$	4.99	25,000	500	18
franklinites	$(Zn,Fe,Mn)(Fe,Mn)_2O_4$	5.21	450,000	8,700	114
Iron Sulfides					
chalcopyrite	$CuFeS_2$	4.20	23–400	0.55–10	16, 114
arsenopyrite	FeAsS	6.05	3,000	50	114
troilite	FeS	4.83	610–1,700	13–36	16, 47, 73
pyrrhotites	$Fe_{1-x}S$	4.62	460–1,400,000	10–30,000	18, 20, 22, 29, 95, 114, 115, 127
pyrrhotite	$Fe_{11}S_{12}$	4.62	1,200	25	16
pyrrhotite	$Fe_{10}S_{11}$	4.62	1,700	38	16
pyrrhotite	Fe_9S_{10}	4.62	170,000	3,800	16
pyrrhotite	Fe_7S_8	4.62	3,200,000	69,000	16
pyrite	FeS_2	5.02	35–5,000	1–100	16, 47, 95, 114
Iron-Titanium Oxides					
hematite	α-Fe_2O_3	5.26	500–40,000	10–760	16, 18, 22, 47, 70, 73, 114, 115
maghemite	γ-Fe_2O_3	4.90	2,000,000–2,500,000	40,000–50,000	1, 115
ilmenite	$FeTiO_3$	4.72	2,200–3,800,000	46–80,000	16, 18, 22, 47, 106, 114, 115
magnetite	Fe_3O_4	5.18	1,000,000–5,700,000	20,000–110,000	16, 18, 22, 55, 61, 62, 75, 114, 115
titanomagnetite	$Fe_{3-x}Ti_xO_4$, x=0.60	4.98	130,000–620,000	2,500–12,000	18, 44, 62
titanomaghemite	$Fe_{(3-x)R}Ti_{xR}\square_{3(1-R)}O_4$, R=8/[8+z(1+x)]	4.99	2,800,000	57,000	22
ulvöspinel	Fe_2TiO_4	4.78	4,800	100	22
Other Iron-Bearing Minerals					
iron	Fe	7.87	3,900,000	50,000	22
goethite	α-FeOOH	4.27	1,100–12,000	26–280	16, 32, 47, 115
lepidocrocite	γ-FeOOH	4.18	1,700–2,900	40–70	16, 47, 115
limonite	$FeOOH{\cdot}nH_2O$	4.20	2,800–3,100	66–74	16, 115

Notes: All susceptibilities were measured in weak fields at room temperature and at one atmosphere pressure. Literature values for susceptibilities were converted to SI units when necessary, and from volume to mass normalization using accepted values for material densities [22, 73, 114]. Susceptibility values have been rounded to the number of significant figures given in the original. Most values come from other tabulations, to which the reader should refer for more information. Values for the more important magnetic minerals (magnetite, titanomagnetite, hematite, pyrrhotite, and goethite) were collated from recent original sources.

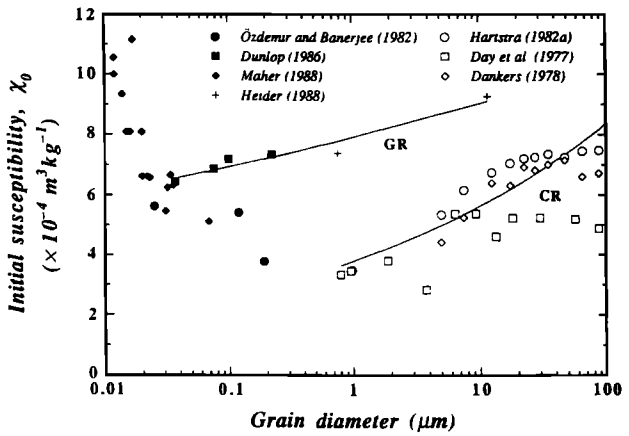

Fig. 1. The grain-size dependence of initial magnetic susceptibility (χ_0) in magnetite. Experimental data from crushed grains (open symbols) and grown crystals (closed symbols and cross). Solid lines are power-law fits for grown (GR) and crushed (CR) samples.

of diamagnetic materials has no temperature dependence. In magnetic materials, there is often a "Hopkinson peak" [e.g., 88] where susceptibility increases just below the Curie temperature before dropping to relatively small values. Examples are shown in Figure 2. The peak occurs at high temperatures because both number and mobility of domain walls in MD grains increase, and thermal activation of SD moments increases, all leading to an increase in response to an external field.

Hydrostatic pressure does not affect the magnitude of magnetic susceptibility in experiments of up to 2 kbar [e.g., 76]. However, uniaxial stress will change the susceptibility both in amount and direction, dependent on the orientation of the applied stress relative to the magnetic field. When the applied stress is parallel to the magnetic field the susceptibility decreases; when the stress and field are perpendicular, there is an increase in magnetic susceptibility [e.g., 82]. The amount of change is reversible, and is dependent both on composition and on magnetic grain size. Changes in susceptibility can be ±40% at 2 kbar of differential stress [76, 82]. However, uniaxial stresses greater than 1–2 kbar are unlikely to be sustained in materials residing at elevated temperatures in the lower crust.

Initial susceptibility is dependent upon the frequency at which it is measured. This is because susceptibility depends on the magnetic domain state of a sample, which in turn depends on the length of time over which the sample is measured or observed. The parameter known as the "frequency dependence of susceptibility" χ_{fd} is usually defined by

$$\chi_{fd} = \frac{\chi_{470Hz} - \chi_{4700Hz}}{\chi_{470Hz}} \times 100\%, \quad (3)$$

where χ_{470Hz} and χ_{4700Hz} are the susceptibility of a sample measured at 470 Hz and that measured at 4700 Hz, respectively. In magnetic materials, there is a small window of grain sizes (near 20 nm in magnetite) which will be magnetically unstable (superparamagnetic) at 470 Hz, but stable (single-domain) at 4700 Hz. Over relatively long "observation times" at 470 Hz, such a grain will appear to be magnetically unstable, and will contribute significantly to the total susceptibility of the sample. But over shorter times at 4700 Hz, the same grain will appear to be stable, and will contribute little to the total susceptibility. A sample containing a significant fraction of such grains will thus have a high value (up to about 12%) of χ_{fd}. This parameter can be used only qualitatively to detect the presence of ultrafine grains of magnetic material such as magnetite or maghemite, which are often found in soils [e.g., 115].

The susceptibility of a sample can also vary with direction, depending on the fabric of the constituent minerals. Anisotropy of magnetic susceptibility (AMS) can be used to determine sedimentary flow directions, or metamorphic deformation parameters [e.g., 57].

3. GRAIN-SIZE DEPENDENCE

Various magnetic properties show a strong grain-size dependence [e.g., 41, 111]. This dependence occurs not because of any intrinsic control of grain size on magnetization, but because these parameters are influenced by the magnetic domain state of the samples, which in turn is a

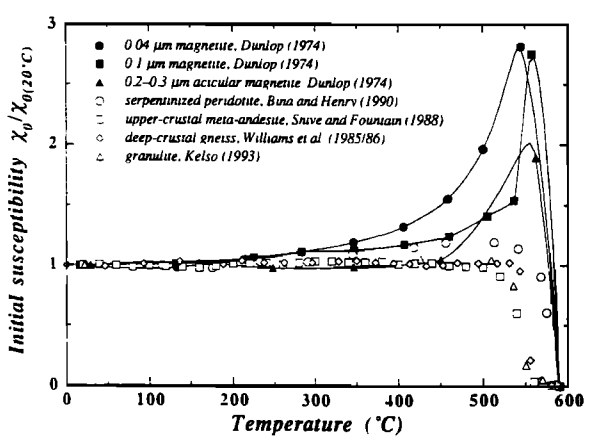

Fig. 2. Temperature dependence of initial magnetic susceptibility (χ_0) for crustal rocks and synthetic fine-grained magnetite. Note the presence of only a very weak Hopkinson peak in the rock data.

function of grain size. Domain states change from superparamagnetic (SPM), to single domain (SD), and finally to multidomain (MD) with increasing grain size. Domain-transition grain sizes depend on composition, temperature, and microstructure. Magnetic granulometry is any magnetic method for determining either the physical or the magnetic grain size of a magnetic material. Magnetic grain size refers to the magnetic domain state and behavior in a magnetic particle, regardless of the physical dimensions of the particle. Here, we are interested in magnetic granulometry of natural magnetic grains, such as magnetite (Fe_3O_4), hematite (α-Fe_2O_3), maghemite (γ-Fe_2O_3), and the various titanium-substituted compositions of these three minerals (titanomagnetite, titanohematite, and titanomaghemite). The composition of the various Fe-Ti oxides and their solid-solution series are shown in Figure 3. These minerals are found in soils, in ocean and lake sediments, and in sedimentary, igneous, and metamorphic rocks.

Both hysteresis and remanence are strongly dependent on grain size. Magnetic hysteresis results when a magnetic mineral is cycled between large positive and negative magnetic field values at room temperature. Remanence properties are measured in a field-free space after a magnetic field has been applied to a sample.

A second category of magnetic granulometry is based on measuring magnetic parameters as a function of temperature, or equivalently, as a function of thermal activation energy/stability. Examples include the frequency dependence of susceptibility discussed above, and low-temperature thermal demagnetization of remanence. In the latter case, remanence acquired at low temperature is lost upon warming, because of the thermal unblocking of magnetic grains, which is dependent on grain size.

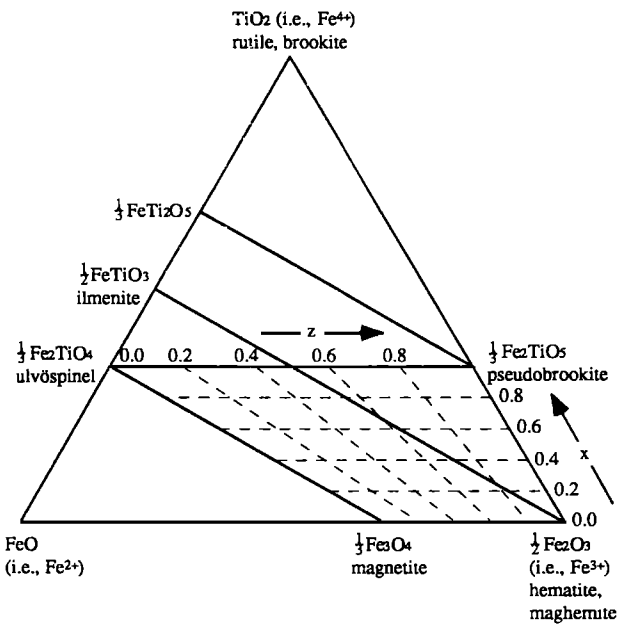

Fig. 3. Ternary diagram of the iron-titanium oxides and their solid-solution series; x is the composition parameter (Ti content) in the titanomagnetite series, and z is the oxidation parameter for titanomaghemites. Figure redrawn from [41].

TABLE 2. Reference Guide for Grain-Size Dependence of Magnetic Parameters

Mineral	References
hematite	25, 30
titanomagnetite	28, 87, 100
titanohematite	125
pyrrhotite	20, 29, 31, 35, 77, 127
goethite	32, 33, 34
maghemite	25

Magnetite has been one of the most extensively studied magnetic minerals, and the important grain-size-dependent hysteresis parameters for this mineral are presented here [e.g., 40]. References for grain-size dependent properties in other minerals systems are listed in Table 2. The grain-size dependence of coercive force (H_c), remanence coercivity (H_{cr}), and reduced saturation remanence (J_{rs}/J_s) for magnetite from various studies are plotted in Figures 4–6. The data, compiled from the literature, are from magnetites that have been synthesized by several different methods: (1) grown crystals (GR) produced either by hydrothermal recrystallization at high temperatures, or by aqueous precipitation at low temperatures [e.g., 3, 40, 55, 75]; (2) crushed grains (CR) produced by crushing and sieving large crystals [e.g., 25, 28, 50]; and (3) glass-ceramic samples (GL) produced by quenching iron-rich glasses from high temperature and then annealing at temperatures below 1000°C [128]. As shown in Figures 4–6, variations in a particular magnetic parameter, such as H_c, for the same nominal grain size are sensitive to the method of sample preparation [e.g., 40], and hence show the importance of microstructure and crystal defects on magnetic behavior. The unique stress-strain histories that different samples have experienced result in different crystal defect populations. For example, hydrothermally recrystallized samples are thought to have low residual strains and a low defect density [55]. In contrast, crushed grains that have been milled have probably undergone extensive brittle/plastic deformation at low temperatures, resulting both in a rapid increase in the number of defects and in a high defect density. The grain-size dependence and magnitude of coercivity, remanence, and susceptibility are important, and are used extensively by environmental magnetists [e.g., 115].

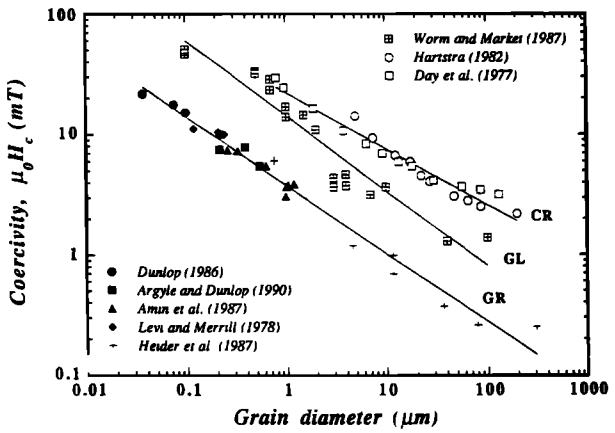

Fig. 4. Grain-size dependence of coercivity (H_c) in magnetite. Experimental data from crushed grains (open symbols), grown crystals (closed symbols and cross), and glass ceramics (hatched symbol). Solid lines are power-law fits for grown (GR), crushed (CR), and glass ceramic (GL) samples.

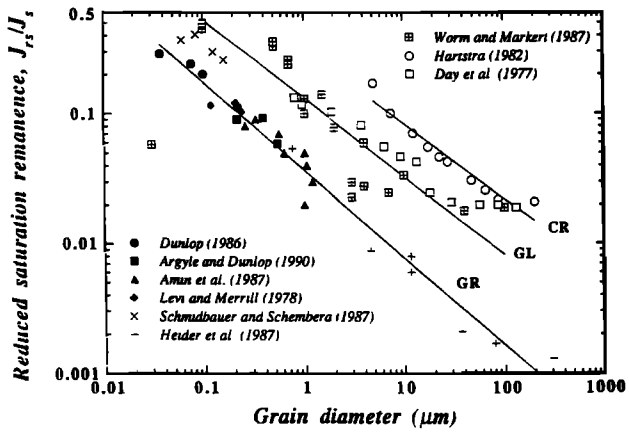

Fig. 6. Grain-size dependence of reduced saturation magnetization (J_{rs}/J_s) in magnetite. Experimental data from crushed grains (open symbols), grown crystals (closed symbols and cross), and glass ceramics (hatched symbol). Solid lines are power-law fits for grown, (GR), crushed (CR), and glass ceramic (GL) samples.

4. INTRINSIC PARAMETERS

4.1. Saturation Magnetization and Curie Temperature

Curie temperatures (T_C) and saturation magnetization (J_s) are intrinsic properties which depend on chemical composition and crystal structure. Saturation magnetization is a function of temperature and disappears at the Curie temperature. Rapid thermomagnetic measurement of T_C aids in determining the composition of magnetic mineral phases.

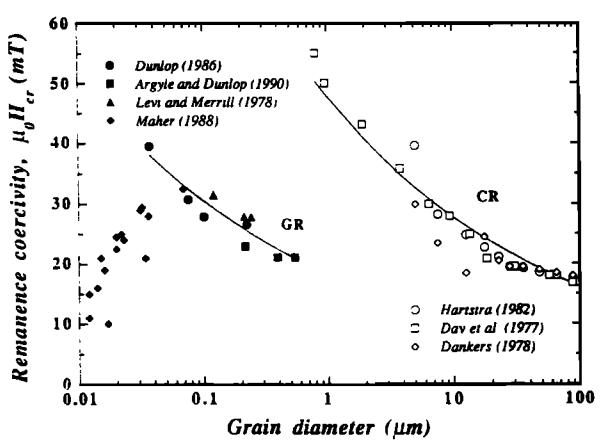

Fig. 5. Grain-size dependence of remanence coercivity (H_{cr}) in magnetite. Experimental data from crushed grains (open symbols) and grown crystals (closed symbols and cross). Solid lines are power-law fits for grown (GR) and crushed (CR) samples.

The composition dependence both of J_s (measured at room temperature) and of T_C for titanomagnetites, titanomaghemites, and titanohematites is shown in Figures 7–9; Table 3 lists T_C and J_s data for other minerals. The thermal dependence of J_s for magnetite and for hematite is given in Table 4 and in Figure 10, respectively.

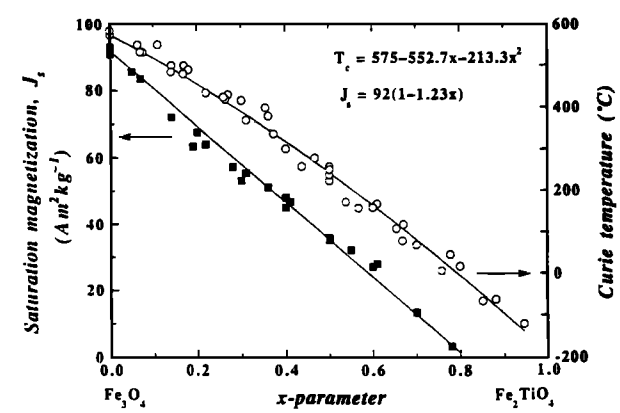

Fig. 7. Variation of room-temperature saturation magnetization (J_s) and Curie temperature (T_C) with composition (x-parameter) in the titanomagnetite ($Fe_{3-x}Ti_xO_4$) solid-solution series. End members are magnetite ($x=0$) and ulvöspinel ($x=1$). Curie temperature data denoted by open circles, and J_s data by solid squares. Solid lines are (1) linear fit to the J_s data [2, 59, 85, 100, 124]; (2) best fit second-order polynomial to T_C data [2, 85, 94, 100, 103, 120]. Best-fit equations are given in the Figure.

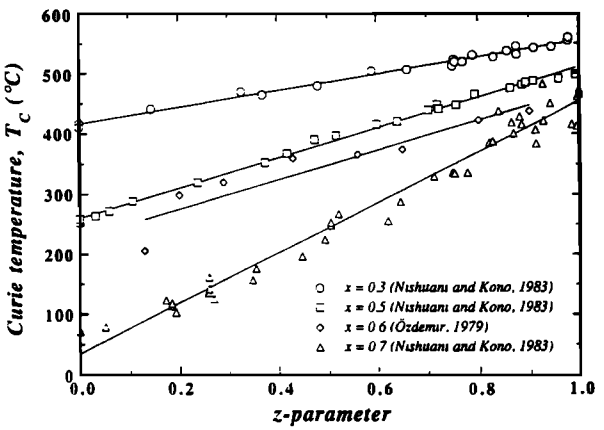

Fig. 8. Variation of Curie temperature (T_C) with degree of oxidation (z-parameter) for the titanomaghemite series ($Fe_{(3-x)R}Ti_{xR}\square_{3(1-R)}O_4$, R = 8/[8+z(1+x)], where □ denotes a lattice vacancy). Solid lines are linear best-fits for each series.

Long-range magnetic ordering below the Curie temperature is achieved by the mechanism of exchange or superexchange interactions, and is usually described by an exchange constant, A [e.g., 24], which is an important parameter in micromagnetic domain theory. From an analysis of a synthesis of published data on inelastic neutron scattering in magnetite [54], the best-fit fourth-order polynomial for the temperature dependence of $A(T)$, useful for reproducing the experimental results, is given by

$$A(T) = (-1.344 + 2.339\times10^{-2}T - 0.706\times10^{-4}T^2 + 8.578\times10^{-8}T^3 - 3.868\times10^{-11}T)\times10^{-11}\ \mathrm{Jm^{-1}}, \quad (4)$$

where T is the absolute temperature.

4.2. Magnetocrystalline Anisotropy

Magnetocrystalline anisotropy and magnetostriction arise from spin-orbit coupling of ionic magnetic moments, resulting in crystallographically controlled easy and hard directions of magnetization [e.g., 11, 24]. The magnetocrystalline anisotropy energy (E_K) for a cubic crystal is given by

$$E_K = K_1(\alpha_1^2\alpha_2^2 + \alpha_2^2\alpha_3^2 + \alpha_3^2\alpha_1^2) + K_2(\alpha_1^2\alpha_2^2\alpha_3^2), \quad (5)$$

where K_1 and K_2 are empirical anisotropy constants, and α's are the direction cosines of magnetization with respect to the principal cubic axes.

For a hexagonal crystal, anisotropy can be expressed in terms of a uniaxial constant that determines the anisotropy between the c-axis and the (0001) plane, and a triaxial constant that determines the in-plane anisotropy perpendicular to the c-axis.

The anisotropy constants depend on mineral composition, crystal structure, temperature, and pressure, but are independent of grain size. Room-temperature values of anisotropy constants for titanomagnetites, maghemite, hematite, and pyrrhotite are listed in Table 5. The values of the anisotropy constants listed in Table 5 were determined for single crystals either by high-field torque measurements [e.g., 45, 46, 113], or by analysis of magnetization curves [e.g., 5, 58]. The temperature dependence both of the basal plane anisotropy constant for hematite, as well as of K_1 for magnetite, are illustrated in Figures 10 and 11, respectively.

4.3. Low-Temperature Magnetic Transitions

Certain magnetic properties may change greatly as a function of temperature below 300 K. Such low-temperature transitions may be diagnostic of mineral composition (see Table 5). In magnetite, there is a crystallographic Verwey phase transition near 118 K [e.g., 11]. Also associated with this transition is a magnetic isotropic point (T_v)—the temperature where K_1 becomes zero as it changes sign, and the characteristic easy directions of magnetization change their orientation (see Figure 11). A remanence given either

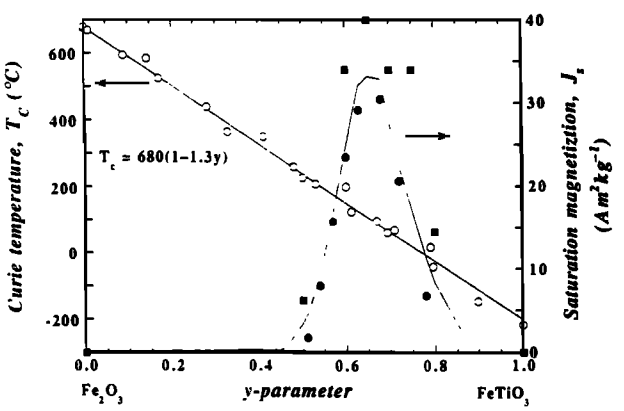

Fig. 9. Variation of room-temperature saturation magnetization (J_s) and Curie temperature (T_C) with composition (y-parameter) in the titanohematite ($Fe_{2-y}Ti_yO_3$) solid-solution series. End members are hematite (y = 0) and ilmenite (y = 1). Curie temperature data is denoted by open symbols, and J_s data by solid symbols. Solid straight line is a linear fit to the T_C data [56, 108, 120]. Best-fit equation is given in the Figure. J_s data from [125, 69]. The complex variation of J_s with composition is due to a change in magnetic ordering from canted antiferromagnetism to ferrimagnetism at $y \cong 0.45$.

TABLE 3. Magnetic Properties of Selected Minerals

Mineral	Composition	Magnetic Order	T_C[a] (°C)	J_s[b] (Am^2kg^{-1})
Oxides				
cobalt ferrite	$CoFe_2O_4$	ferrimagnetic	520	80
copper ferrite	$CuFe_2O_4$	ferrimagnetic	455	25
hematite	α-Fe_2O_3	canted antiferromagnetic	675	0.4
maghemite	γ-Fe_2O_3	ferrimagnetic	~600	70–80
ilmenite	$FeTiO_3$	antiferromagnetic	-233	
magnetite	Fe_3O_4	ferrimagnetic	575–585	90–92
ulvöspinel	Fe_2TiO_4	antiferromagnetic	-153	
magnesioferrite	$MgFe_2O_4$	ferrimagnetic	440	21
jacobsite	$MnFe_2O_4$	ferrimagnetic	~300	77
trevorite	$NiFe_2O_4$	ferrimagnetic	585	51
Sulfides				
troilite	FeS	antiferromagnetic	305	
pyrrhotite	Fe_7S_8	ferrimagnetic	320	20
greigite	Fe_3S_4	ferrimagnetic	~333	~25
Oxyhydroxides				
goethite	α-FeOOH	antiferromagnetic/weak ferromagnetic	~120	<1
feroxyhyte	δ-FeOOH	ferrimagnetic	~180	<10
lepidocrocite	γ-FeOOH	antiferromagnetic(?)	-196	
Metals and Alloys				
cobalt	Co	ferromagnetic	1131	161
wairauite	CoFe	ferromagnetic	986	235
iron	Fe	ferromagnetic	770	218
nickel	Ni	ferromagnetic	358	55
awaruite	Ni_3Fe	ferromagnetic	620	120

[a] T_C = Curie temperature (ferromagnetic materials) or Néel temperature (ferrimagnetic and antiferromagnetic materials).
[b] J_s = Saturation magnetization at room temperature.
References: [24, 78, 115].

above or below this transition will be reduced upon passing through T_v. In hematite, the transition is called the Morin transition and occurs near 263 K in bulk samples, but is suppressed in fine grains less than 20 nm because of internal dilatational strain [84]. A newly discovered transition in pyrrhotite occurs near 34 K [35, 101], but its microscopic cause is unknown. All these transition temperatures are known to be sensitive to impurities, grain size, and non-stoichiometry; in some cases, the transition can be totally suppressed [e.g., 6, 11, 111]. Thus, low-temperature remanence transitions for mineral identification should be used with caution. Depending on the type of experiment, a distinction is made in Table 5 between isotropic points (T_v), where K_1 becomes zero, and remanence transitions (T_R), where a change in remanence or susceptibility occurs.

4.4. Magnetostriction

Magnetostriction is the change in crystal dimensions that accompanies the process of magnetization, and can be defined as the strain dependence of magnetocrystalline anisotropy. The linear saturation magnetostriction constant λ is the fractional change in length $\Delta\ell/\ell$ of a material when it is magnetized from a demagnetized state to saturation. It can be positive (elongation) or negative (contraction), and it is usually anisotropic in single crystals. The microscopic origin of magnetostriction is the same spin-orbit coupling that produces magnetocrystalline anisotropy [e.g., 24].

In cubic crystals, the linear magnetostriction λ is described by the two-constant expression [e.g., 24],

$$\lambda = \tfrac{3}{2}\lambda_{100}(\alpha_1^2\beta_1^2 + \alpha_2^2\beta_2^2 + \alpha_3^2\beta_3^2 - \tfrac{1}{3}) + 3\lambda_{111}(\alpha_1\alpha_2\beta_1\beta_2 + \alpha_2\alpha_3\beta_2\beta_3 + \alpha_1\alpha_3\beta_1\beta_3), \quad (6)$$

where λ is the strain measured in the direction defined by direction cosines β_i, and α_i are the direction cosines of the magnetization. Both β_i and α_i (i = 1, 2, 3) are measured relative to the principal cubic axes. The magnetostriction

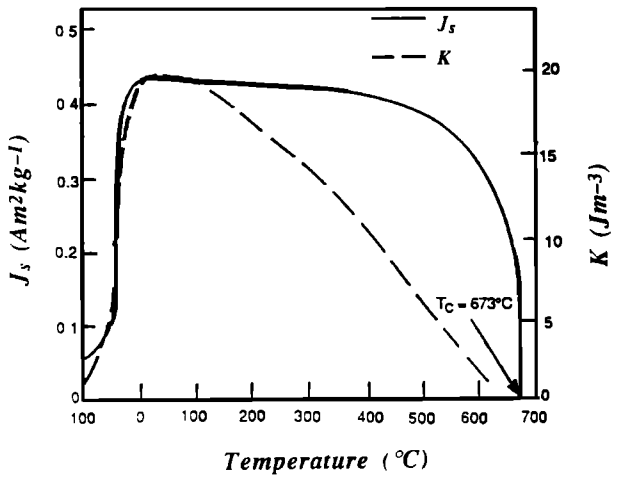

Fig. 10. Variation of saturation magnetization (J_s) and basal plane anisotropy constant (K) with temperature for a natural crystal of hematite from Ascension. Note the effect of the Morin transition below –10°C. Figure modified after [11, 45].

constants along the <100> and <111> crystal directions are λ_{100} and λ_{111}, respectively. A related parameter is the polycrystalline magnetostriction constant λ_s, given by

$$\lambda_s = \frac{3}{5}\lambda_{100} + \frac{2}{5}\lambda_{111}. \quad (7)$$

Like the magnetocrystalline anisotropy constants, magnetostriction constants vary as a function of composition, crystal structure, temperature, and pressure. Room-temperature values of single-crystal and polycrystal magnetostriction constants for titanomagnetites, maghemite, hematite, and pyrrhotite are listed in Table 5. The temperature dependence of the magnetostriction constants for magnetite is shown in Figure 12.

4.5. Pressure Dependence

Only a weak hydrostatic pressure dependence of magnetocrystalline anisotropy, magnetostriction, and Curie temperature has been detected in magnetite. The results of one study [83] were that K_1 and K_2 decrease with pressure at the rate of –0.05%/MPa (–5%/kbar), whereas λ_{100} and λ_{111} increase at the rate of +0.15%/MPa (15%/kbar). The results of another [105] were that the Curie temperature for magnetite and for various titanomagnetites increases with pressure at approximately 0.02 K/MPa (2 K/kbar).

5. REMANENCES

Remanent magnetization is the permanent magnetization of a sample in the absence of an external magnetic field, and thus occurs only in materials which exhibit hysteresis. A remanence can be a volume magnetization (magnetic moment per volume, measured in units of Am^{-1}), or a mass magnetization (magnetic moment per mass, measured in units of Am^2kg^{-1}).

Thermal remanent magnetization (TRM) is the remanence acquired by a sample when it cools to room temperature starting at or above its Curie/Néel point in the presence of an external magnetic field (usually 50–100 μT). TRM is often used as a laboratory model for the acquisition of

TABLE 4. Temperature Dependence of Saturation Magnetization in Magnetite

Absolute Temperature T (K)	Saturation Magnetization J_s^* (Am^2kg^{-1})
20.4	98.80
77.1	98.37
284.6	92.14
325.2	90.36
372.7	87.49
415.9	84.82
452.3	82.15
498.9	78.40
539.5	74.84
586.1	69.99
631.0	64.85
678.4	58.82
728.4	51.51
761.5	45.18
790.3	37.86
830.1	22.54

*J_{s0} = 98.86 Am^2kg^{-1} at absolute zero. Reference: [96].

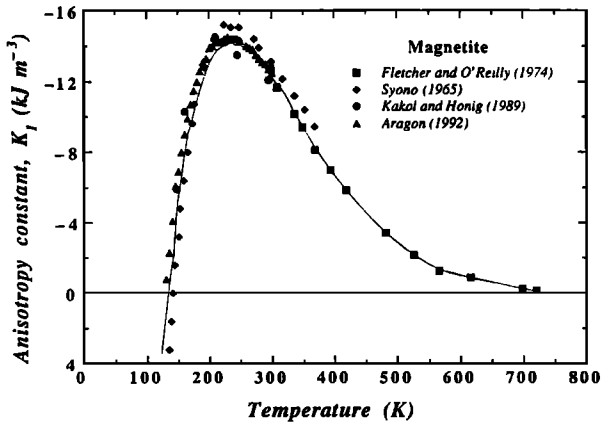

Fig. 11. Variation of first-order magnetocrystalline anisotropy constant (K_1) of magnetite with absolute temperature.

TABLE 5. Room-Temperature Values of Magnetocrystalline and Magnetostriction Constants

Mineral	K_1 ($\times 10^4$ Jm^{-3})	K_2 ($\times 10^4$ Jm^{-3})	λ_{111} ($\times 10^{-6}$)	λ_{100} ($\times 10^{-6}$)	λ_s ($\times 10^{-6}$)	T_v[a] (K)	T_R[a] (K)	References
Titanomagnetites								
Fe_3O_4 [TM0]	–1.23[b]	0.44	78	–20	39	120–130	118	5, 6, 47, 60, 113
TM04	–1.94[c]	–0.18[c]	87	–6	50	112		113
TM05	–1.5	0.2				95*		60
TM10	–2.50	0.48	96	4	59.2	92		113
TM18	–1.92		109	47	84.2			113
TM19	–2.04	1.0				<50		60
TM28	–1.92	–0.3				<50		60
TM31	–1.81		104	67	89.2			113
TM36	–1.6	0.3				68*		60
TM40			148.2	146.5	147.5			68
TM40 (PC)[d]					122.7			80
TM41	–1.4	0.3				125		60
TM52							133	117
TM55	≈0	1.4						60
TM56	–0.70					228		113
TM59							211	117
TM60			79.3	137.9	102.7			68
TM60 (PC)[d]					111.3			80
TM60							243	117
TM65							262	117
TM68	0.18					≈300		113
TM70			9.3	65.4	31.7			68
Other Minerals								
γ-Fe_3O_4	–0.46 (SCF)[d]				–(5–10) (PC)[d]	None	None	12
α-Fe_2O_3	7–188$\times 10^{-5}$[e]				≈8	263		45, 79
Fe_7S_8	11.8[f]	32.2[f]			<10[g]		35	14, 31, 110

Notes: An asterisk indicates an extrapolated value.
[a]T_v is temperature where $K_1 = 0$, T_R is temperature where a change in remanence or susceptibility occurs.
[b]Average value from listed references.
[c]Data from [60], which have the following error limits: K_1 ±5%, K_2 ±20%.
[d]PC = polycrystalline sample, SCF = single crystal thin film.
[e]In-plane anisotropy constant.
[f]K_3 and K_4 anisotropy constants.
[g]Based on domain observations [110].

remanence by magnetic minerals in newly-formed igneous rocks which cool through their Curie temperatures in the Earth's field. Experimental studies have been made on TRM as a function of grain size for magnetite (see Figure 13), and as a function of composition in titanomagnetites [e.g., 26, 87, 93, 100, 119], in titanomaghemites [e.g., 86, 89], and in titanohematites [e.g., 69, 120]. Reverse TRM has been found for certain compositions of titanohematite (see Figure 14).

Anhysteretic remanent magnetization (ARM) is a laboratory remanence acquired by a sample at room temperature during treatment in an decaying, alternating magnetic field (peak field about 100 mT) with a superimposed steady field (usually 50–100 μT). ARM has been used as an analog for TRM, but avoids the possibility of altering the magnetic minerals at high temperature. It is also commonly used in environmental magnetism for magnetic granulometry [e.g., 115]. The results of several studies of the grain-size dependence of ARM in magnetite are plotted in Figure 15.

Isothermal remanent magnetization (IRM) is a laboratory remanence acquired by a sample at after exposure to a steady external magnetic field at a given temperature. If the external field is strong enough to saturate the magnetic minerals in the sample (typically 1 T), then the remanence is

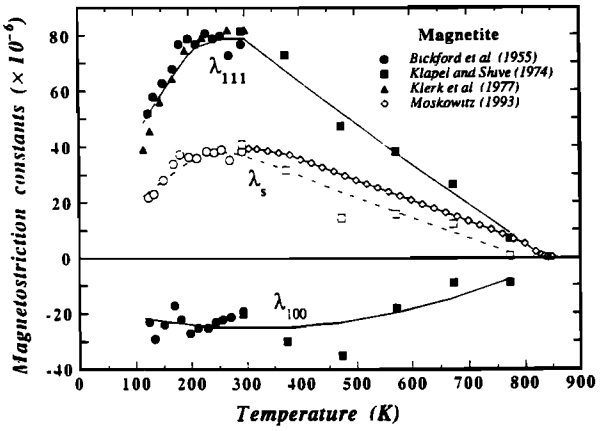

Fig. 12. Variation of magnetostriction constants (λ_{111}, λ_{100}, and λ_s) for magnetite with absolute temperature. Single crystal data from [13,67,68]; polycrystalline data from [80]. λ_s calculated from single crystal data or measured directly by [80].

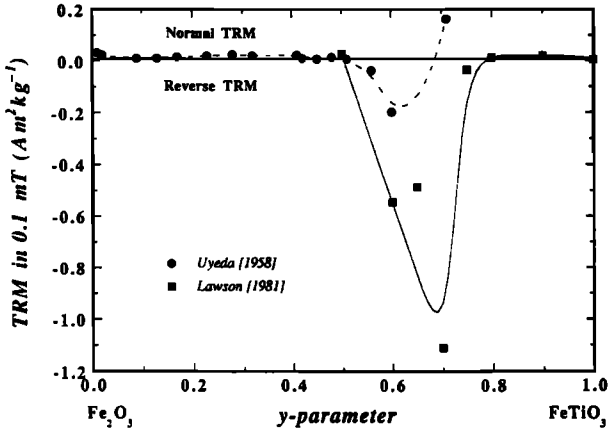

Fig. 14. Variation of weak-field TRM intensity with composition (y-parameter) for titanohematites ($Fe_{2-y}Ti_yO_3$). Note the reverse TRM acquired when titanium content is in the range 0.55 to 0.75. TRM data have been normalized to an induction field of to 0.1 mT (80 Am^{-1}, or 1 Oe).

called a saturation isothermal remanent magnetization (SIRM). SIRM is essentially the same as J_{rs} from a hysteresis loop. Variations in IRM and SIRM are related to the coercivity spectrum of a sample, and can thus be used for magnetic mineralogy determinations in environmental magnetism studies [e.g., 65].

Natural remanent magnetization (NRM) is the remanence in a rock before any demagnetization treatment in the laboratory. It is usually acquired parallel to the Earth's magnetic field at the time of formation or alteration. NRM is the most variable of magnetic parameters because it depends not only on mineralogy and grainsize, but also on the mode of remanence acquisition, and on thermal and magnetic history. Nevertheless, NRM is a critical parameter in crustal magnetization studies that try to model the sources of marine and continental magnetic anomalies. A summary of several models of oceanic crust magnetization is shown in Figure 16 [116].

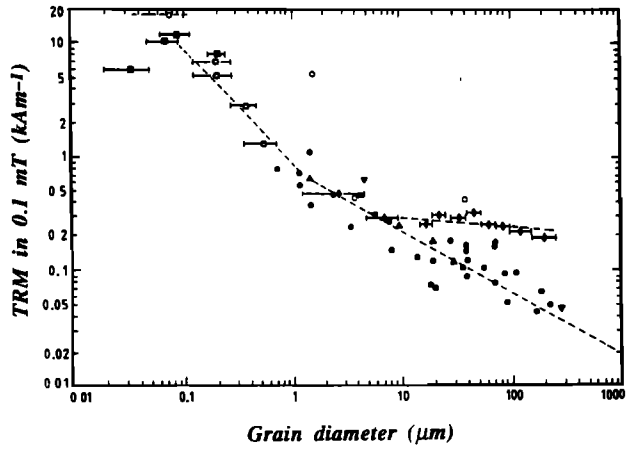

Fig. 13. Grain-size dependence of weak-field thermal remanent magnetization (TRM) intensity for magnetite. Data from crushed grains (> 1 μm), grown crystals (< 1 μm), and magnetite of other origins compiled by [41]. See original paper for references. Figure modified after [41].

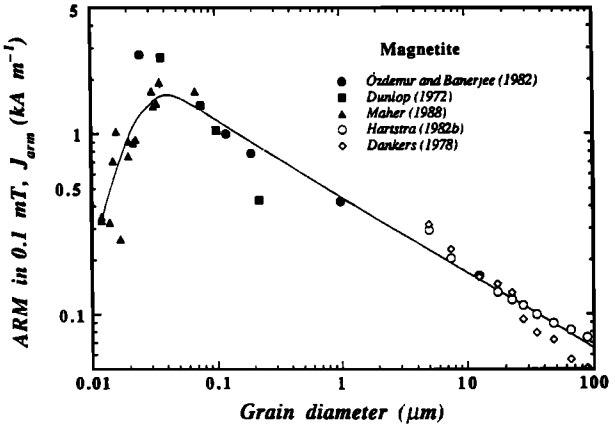

Fig. 15. Grain-size dependence of weak-field anhysteretic remanent magnetization (ARM) intensity for magnetite. Experimental data from crushed grains (open symbols) and grown crystals (closed symbols). ARM data have been normalized to an induction field of 0.1 mT (80 Am^{-1}, or 1 Oe).

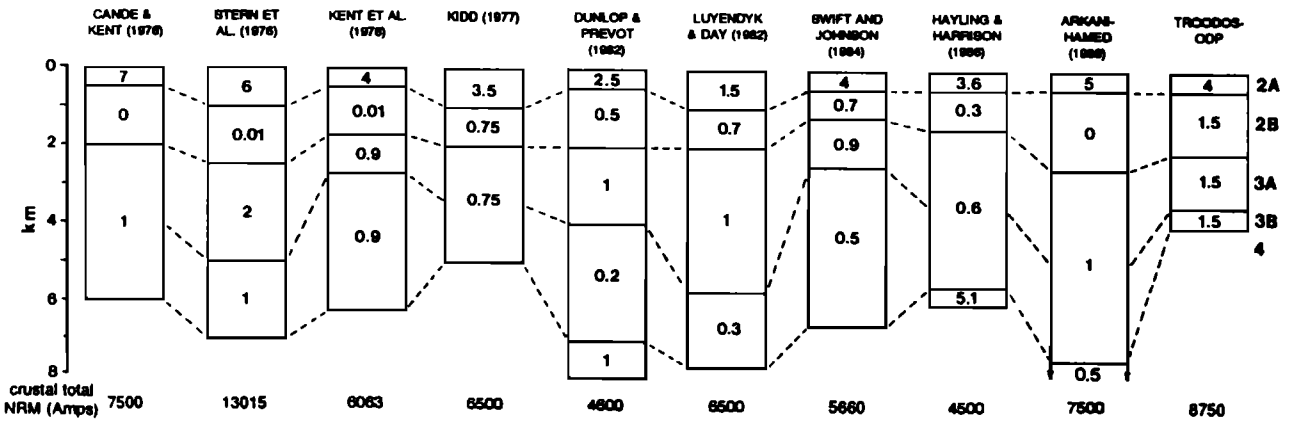

Fig. 16. Models of natural remanent magnetization (NRM) in the oceanic crust. Seismic layers are identified at right. NRM values within layers are in Am^{-1}. Values at the bottom of columns are the crustal total NRM in amperes, neglecting values from below the Moho. See original paper for references. Figure from [116].

TABLE 6. Koenigsberger Ratios for Selected Rocks

Rocks	Koenigsberger Ratio, Q_n	References
Sedimentary Rocks		
marine sediments	5	18
red sediments	1.6–6	18
siltstone	0.02–2	18
silty shale	5	18
avg sedimentary rocks	0.02–10	18, 107
Igneous Rocks		
granite	0.1–28	18, 107
granodiorite	0.1–0.2	18, 107
dolerite	2–3.5	18, 107
diabase	0.2–4	18, 107
gabbro	1–9.5	18, 107
oceanic gabbro	0.1–58.4	66
intrusions	0.1–20	18, 107
volcanics	30–50	18
subaerial basalt	1–116	18, 98
oceanic basalt	1–160	18, 107
seamounts	8–57	107
avg igneous rocks	1–40	18
Metamorphic Rocks		
granulites	0.003–50	63, 116, 122
Others		
magnetite ore	1–94	18, 107
manganese ore	1–5	107
lunar rocks	0.001–1	18

TABLE 7. Reference Guide for Other Remanences

Remanence	References
Chemical (CRM)	17, 48, 64, 91, 92, 97, 112
Depositional (DRM)	4, 7, 8, 71
Viscous (VRM)	10, 39, 43, 49

The relative importance of NRM compared with induced magnetization is characterized by the Koenigsberger ratio Q_n, a dimensionless quantity given by

$$Q_n = \mathrm{NRM} / kH_e, \tag{8}$$

where NRM is the magnitude of the natural remanent magnetization (per unit volume), k is the volume susceptibility, and H_e is the magnitude of the Earth's magnetic field at the site under consideration ($H_e = 24$–$48\ \mathrm{Am}^{-1}$, $B_e = \mu_0 H_e = 30$–$60\ \mu\mathrm{T}$). Values of Q_n for several rock types are collected in Table 6.

Other types of remanence—including chemical (CRM), depositional (DRM), viscous (VRM)—have also been the subject of extensive study, but are not included here. The interested reader can refer to the papers cited in Table 7 for further discussion.

Acknowledgements. Thanks are due to Paul Kelso for helpful input. This is contribution number 9301 of the Institute for Rock Magnetism (IRM). The IRM is funded by the W. M. Keck Foundation, the National Science Foundation, and the University of Minnesota.

REFERENCES

1. Adnan, J., A. de Sa, and W. O'Reilly, Simultaneous measurement of the variations in the magnetic susceptibility and remanence of materials in the temperature range 10–700°C and at elevated pressure (16–160 MPa), *Meas. Sci. Technol.*, *3*, 289-295, 1992.
2. Akimoto, S., Magnetic properties of FeO–Fe_2O_3–TiO_2 system as a basis of rock magnetism, *J. Phys. Soc. Jpn.*, *17, suppl. B1*, 706-710, 1962.
3. Amin, N., S. Arajs, and E. Matijevic, Magnetic properties of uniform spherical magnetic particles prepared form ferrous hydroxide gels, *Phys. Stat. Sol. A*, *101*, 233-238, 1987.
4. Anson, G. L., and K. P. Kodama, Compaction-induced inclination shallowing of the post-depositional remanent magnetization in a synthetic sediment, *Geophys. J. R. Astr. Soc.*, *88*, 673-692, 1987.
5. Aragón, R., Cubic magnetic anisotropy of nonstoichiometric magnetite, *Phys. Rev. B*, *46*, 5334-5338, 1992.
6. Aragón, R., D. J. Buttrey, J. P. Shepherd, and J. M. Honig, Influence of nonstoichiometry on the Verwey transition, *Phys. Rev. B*, *31*, 430-436, 1985.
7. Arason, P., and S. Levi, Compaction and inclination shallowing in deep-sea sediments from the Pacific Ocean, *J. Geophys. Res.*, *95B*, 4501-4510, 1990*a*.
8. Arason, P., and S. Levi, Models of inclination shallowing during sediment compaction, *J. Geophys. Res.*, *95B*, 4481-4500, 1990*b*.
9. Argyle, K. S., and D. J. Dunlop, Low-temperature and high-temperature hysteresis of small multidomain magnetites (215–540 nm), *J. Geophys. Res.*, *95B*, 7069-7083, 1990.
10. Arkani-Hamed, J., Thermoviscous remanent magnetization of oceanic lithosphere inferred from its thermal evolution, *J. Geophys. Res.*, *94B*, 17,421-17,436, 1989.
11. Banerjee, S. K., Magnetic properties of Fe-Ti oxides, in *Oxide Minerals: Petrologic and Magnetic Significance*, vol. 25, edited by D. H. Lindsley, pp. 107-128, Mineralogical Society of America, Reviews in Mineralogy, Washington, 1991.
12. Bate, G., Recording materials, in *Ferromagnetic Materials*, *2*, edited by E. P. Wohlfarth, pp. 381-507, Elsevier North-Holland, New York, 1980.
13. Bickford, L. R., Jr., J. Pappis, and J. Stull, Magnetostriction and permeability of magnetite and cobalt-substituted magnetite, *Phys. Rev.*, *99*, 1210-1214, 1955.
14. Bin, M., and R. Pauthenet, Magnetic anisotropy in pyrrhotite, *J. Appl. Phys.*, *34*, 1161-1162, 1963.
15. Bina, M. M., and B. Henry, Magnetic properties, opaque mineralogy, and magnetic anisotropies of serpentinized peridotites from ODP Hole 670A near the mid-Atlantic ridge, *Phys. Earth Planet. Inter.*, *65*, 88-103, 1990.
16. Bleil, U., and N. Petersen, Magnetic properties, in *Landolt-Börnstein Numerical Data and Functional Relationships in Science and Technology; Group V: Geophysics and Space Research; vol. 1b, Physical Properties of Rocks*, edited by G. Angenheister, pp. 308-432, Springer-Verlag, New York, 1982.
17. Brown, K., and W. O'Reilly, The effect of low temperature oxidation on the remanence of TRM-carrying titanomagnetite $Fe_{2.4}Ti_{0.6}O_4$, Phys. Earth Planet. Inter., 52, 108-116, 1988.
18. Carmichael, R. S. (Ed.), *Practical Handbook of Physical Properties of Rocks and Minerals*, 741 pp., CRC Press, Boca Raton, FL, 1989.
19. Clark, D. A., Comments on magnetic petrophysics, *Bull. Aust. Soc. Explor. Geophys.*, *14*, 49-62, 1983.
20. Clark, D. A., Hysteresis properties of sized dispersed monoclinic pyrrhotite grains, *Geophys. Res. Lett.*, *11*, 173-176, 1984.
21. Coey, J. M. D., Magnetic properties of iron in soil iron oxides and clay minerals, in *Iron in Soils and Clay Minerals*, edited by J. W. Stucki, B. A. Goodman, and U. Schwertmann, pp. 397-466, Reidel Publishing, Dordrecht, 1988.
22. Collinson, D. W., *Methods in Rock Magnetism and Palaeomagnetism: Techniques and Instrumentation*, vol. 11, 503 pp., Chapman and Hall, New York, 1983.
23. Craik, D. J., *Structure and Properties of Magnetic Materials*, 244 pp., Pion, Ltd., London, 1971.
24. Cullity, B. D., *Introduction to Magnetic Materials*, 666 pp., Addison-Wesley, Reading, MA, 1972.
25. Dankers, P. H. M., Magnetic properties of dispersed natural iron-oxides of known grain-size, Ph. D. Dissertation, University of Utrecht, 1978.
26. Day, R., The effect of grain size on the magnetic properties of the magnetite–ulvöspinel solid solution series, Ph. D. Dissertation, University of Pittsburgh, 1973.
27. Day, R., TRM and its variation with grain size: a review, *J. Geomagn. Geoelectr.*, *29*, 233-265, 1977.
28. Day, R., M. Fuller, and V. A. Schmidt, Hysteresis properties of titanomagnetites: grain-size and compositional dependence, *Phys. Earth Planet. Inter.*, *13*, 260-266, 1977.
29. Dekkers, M. J., Magnetic properties of natural pyrrhotite Part I: Behaviour of initial susceptibility and saturation-magnetization-related rock-magnetic parameters in a grain-size dependent framework, *Phys. Earth Planet. Inter.*, *52*, 376-393, 1988.
30. Dekkers, M. J., Rock magnetic properties of fine-grained natural low-temperature haematite with reference to remanence acquisition mechanisms in red beds, *Geophys. J. Int.*, *99*, 1-18, 1989*a*.
31. Dekkers, M. J., Magnetic properties of natural pyrrhotite. II. High- and low-temperature behavior of J_n and TRM as a function of grain size, *Phys. Earth Planet. Inter.*, *57*, 266-283, 1989*b*.
32. Dekkers, M. J., Magnetic properties of natural goethite—I. Grain-size dependence of some low- and high-field related rock magnetic parameters measured at room temperature, *Geophys. J.*, *97*, 323-340, 1989*c*.
33. Dekkers, M. J., Magnetic properties of natural goethite—II. TRM behaviour during thermal and alternating field demagnetization and low-temperature treatment, *Geophys. J.*, *97*, 341-355, 1989*d*.
34. Dekkers, M. J., Magnetic properties of natural goethite—III. Magnetic behaviour and properties of minerals originating from goethite dehydration

during thermal demagnetization, *Geophys. J. Int.*, *103*, 233-250, 1990.

35. Dekkers, M. J., J.-L. Mattéi, G. Eillon, and P. Rochette, Grain-size dependence of the magnetic behavior of pyrrhotite during its low-temperature transition at 34K, *Geophys. Res. Lett.*, *16*, 855-858, 1989.
36. Dunlop, D. J., Grain-size dependence of anhysteresis in iron oxide micropowders, *IEEE Trans. Magn.*, *MAG-8*, 211-213, 1972.
37. Dunlop, D. J., Thermal enhancement of magnetic susceptibility, *J. Geophys.*, *40*, 4339-4351, 1974.
38. Dunlop, D. J., The rock magnetism of fine particles, *Phys. Earth Planet. Inter.*, *26*, 1-26, 1981.
39. Dunlop, D. J., Viscous magnetization of 0.04–100 μm magnetites, *J. Geophys.*, *74*, 667-687, 1983.
40. Dunlop, D. J., Hysteresis properties of magnetite and their dependence on particle size: a test of pseudo-single-domain remanence models, *J. Geophys. Res.*, *91B*, 9569-9584, 1986.
41. Dunlop, D. J., Developments in rock magnetism, *Rep. Prog. Phys.*, *53*, 707-792, 1990.
42. Dunlop, D. J., and K. S. Argyle, Thermoremanence and anhysteretic remanence of small multidomain magnetites, *J. Geophys. Res.*, *95B*, 4561-4577, 1990.
43. Dunlop, D. J., and Ö. Özdemir, Alternating field stability of high-temperature viscous remanent magnetization, *Phys. Earth Planet. Inter.*, *65*, 188-196, 1990.
44. Dunlop, D. J., Ö. Özdemir, and R. J. Enkin, Multidomain and single-domain relations between susceptibility and coercive force, *Phys. Earth Planet. Inter.*, *49*, 181-191, 1987.
45. Flanders, P. J., and W. J. Scheuele, Temperature-dependent magnetic properties of hematite single crystals, Proceedings of the International Conference on Magnetism, Nottingham, U. K., 1964.
46. Fletcher, E. J., and W. O'Reilly, Contribution of Fe^{2+} ions to the magnetocrystalline anisotropy constant K_1 of $Fe_{3-x}Ti_xO_4$ ($0 < x < 0.1$), *J. Phys. C*, *7*, 171-178, 1974.
47. Foëx, G., C.-J. Gorter, and L.-J. Smits, *Constantes Sélectionées: Diamagnétisme et Paramagnétisme; Relaxation Paramagnétique*, vol. 7, 317 pp., Union Internationale de Chimie, Masson & Cie., Paris, 1957.
48. Gapeev, A. K., S. K. Gribov, D. J. Dunlop, Ö. Özdemir, and V. P. Shcherbakov, A direct comparison of the properties of CRM and VRM in the low-temperature oxidation of magnetites, *Geophys. J. Int.*, *105*, 407-418, 1991.
49. Halgedahl, S. L., Experiments to investigate the origin of anomalously elevated unblocking temperatures, *J. Geophys. Res., in press*, 1993.
50. Hartstra, R. L., Grain-size dependence of initial susceptibility and saturation magnetization-related parameters of four natural magnetites in the PSD-MD range, *Geophys. J. R. Astr. Soc.*, *71*, 477-495, 1982*a*.
51. Hartstra, R. L., A comparative study of the ARM and I_{rs} of some natural magnetites of MD and PSD grain size, Geophys. *J. R. Astr. Soc.*, *71*, 497-518, 1982*b*.
52. Hartstra, R. L., TRM, ARM, and I_{rs} of two natural magnetites of MD and PSD grain size, *Geophys. J. R. Astr. Soc.*, *73*, 719-737, 1983.
53. Heider, F., Magnetic properties of hydrothermally grown Fe_3O_4 crystals, Ph. D. Dissertation, University of Toronto, 1988.
54. Heider, F., and W. Williams, Note on temperature dependence of exchange constant in magnetite, *Geophys. Res. Lett.*, *15*, 184-187, 1988.
55. Heider, F., D. J. Dunlop, and N. Sugiura, Magnetic properties of hydrothermally recrystallized magnetite crystals, *Science*, *236*, 1287-1290, 1987.
56. Ishikawa, Y., and S. Akimoto, Magnetic properties of the $FeTiO_3$–Fe_2O_3 solid solution series, *J. Phys. Soc. Jpn.*, *12*, 1083-1098, 1957.
57. Jackson, M. J., and L. Tauxe, Anisotropy of magnetic susceptibility and remanence: developments in the characterization of tectonic, sedimentary, and igneous fabric, *Rev. Geophys.*, *29, suppl. (IUGG Report–Contributions in Geomagnetism and Paleomagnetism)*, 371-376, 1991.
58. Kakol, Z., and J. M. Honig, Influence of deviations from ideal stoichiometry on the anisotropy parameters of magnetite $Fe_{3(1-\delta)}O_4$, *Phys. Rev. B*, *40*, 9090-9097, 1989.
59. Kakol, Z., J. Sabol, and J. M. Honig, Cation distribution and magnetic properties of titanomagnetites $Fe_{3-x}Ti_xO_4$ ($0 \quad x < 1$), *Phys. Rev. B*, *43*, 649-654, 1991*a*.
60. Kakol, Z., J. Sabol, and J. M. Honig, Magnetic anisotropy of titanomagnetites $Fe_{3-x}Ti_xO_4$, $0 \quad x \quad 0.55$, *Phys. Rev. B*, *44*, 2198-2204, 1991*b*.
61. Kapicka, A., Magnetic susceptibility under hydrostatic pressure of synthetic magnetite samples, *Phys. Earth Planet. Inter.*, *70*, 248-252, 1992.
62. Kean, W. F., R. Day, M. Fuller, and V. A. Schmidt, The effect of uniaxial compression on the initial susceptibility of rocks as a function of grain size and composition of their constituent titanomagnetites, *J. Geophys. Res.*, *81*, 861-872, 1976.
63. Kelso, P. R., S. K. Banerjee, and C. Teyssier, The rock magnetic properties of the Arunta Block, central Australia and their implication for the interpretation of long wavelength magnetic anomalies, *J. Geophys. Res., in press*, 1993.
64. Kelso, P. R., S. K. Banerjee, and H.-U. Worm, The effect of low-temperature hydrothermal alteration on the remanent magnetization of synthetic titanomagnetites: a case for the acquisition of chemical remanent magnetization, *J. Geophys. Res.*, *96B*, 19,545-19,553, 1991.
65. King, J. W., and J. E. T. Channell, Sedimentary magnetism, environmental magnetism, and magnetostratigraphy, *Rev. Geophys., 29, suppl. (IUGG Report–Contributions in Geomagnetism and Paleomagnetism)*, 358-370, 1991.
66. Kikawa, E., and J. Pariso, Magnetic properties of gabbros from hole 735B at the Southwest Indian Ridge, *Proc. ODP Sci. Res.*, *118*, 285-307, 1991.
67. Klapel, G. D., and P. N. Shive, High-temperature magnetostriction of magnetite, *J. Geophys. Res.*, *79*, 2629-2633, 1974.
68. Klerk, J., V. A. M. Brabers, and A. J. M. Kuipers, Magnetostriction of the mixed series $Fe_{3-x}Ti_xO_4$, *J. Phys., 38 C1*, 87-189, 1977.

University, 1981.

70. Lefever, R. A., Fe oxides and Fe-Me-O compounds, in *Landolt-Börnstein Numerical Data and Functional Relationships in Science and Technology; Group III: Crystal and Solid State Physics; vol. 12b, Magnetic and Other Properties of Oxides and Related Compounds*, edited by K.-H. Hellwege and A. M. Hellwege, pp. 1-53, Springer-Verlag, New York, 1980.
71. Levi, S., and S. K. Banerjee, On the origin of inclination shallowing in redeposited sediments, *J. Geophys. Res., 95B*, 4383-4390, 1990.
72. Levi, S., and R. T. Merrill, Properties of single domain, pseudo-single domain, and multidomain magnetite, *J. Geophys. Res., 83B*, 309-323, 1978.
73. Lide, D. R. (Ed.), *CRC Handbook of Chemistry and Physics*, 73rd ed., CRC Press, Boca Raton, FL, 1992.
74. Lindsley, D. H., G. E. Andreasen, and J. R. Balsley, Magnetic properties of rocks and minerals, in *Handbook of Physical Constants, Memoir 97*, edited by S. P. Clark, pp. 543-552, Geological Society of America, New York, 1966.
75. Maher, B. A., Magnetic properties of some synthetic submicron magnetites, *Geophys. J., 94*, 83-96, 1988.
76. Martin, R. J., III, Is piezomagnetism influenced by microcracks during cyclic loading?, *J. Geomagn. Geoelectr., 32*, 741-755, 1980.
77. Menyeh, A., and W. O'Reilly, The magnetization process in monoclinic pyrrhotite (Fe_7S_8) particles containing few domains, *Geophys. J. Int., 104*, 387-399, 1991.
78. Merrill, R. T., and M. W. McElhinny, *The Earth's Magnetic Field: Its History, Origin, and Planetary Perspective*, vol. 32, 401 pp., Academic Press, Orlando, 1983.
79. Mizushima, K. T., and K. Iida, Effective in-plane anisotropy field in α-Fe_2O_3, *J. Phys. Soc. Jpn., 26*, 1521-1526, 1969.
80. Moskowitz, B. M., High-temperature magnetostriction of magnetite and titanomagnetites, *J. Geophys. Res., 98B*, 359-371, 1993.
81. Nagata, T., *Rock Magnetism*, 2nd ed., 350 pp., Maruzen, Tokyo, 1961.
82. Nagata, T., Basic magnetic properties
69. Lawson, C. A., Magnetic and microstructural properties of minerals of the ilmenite-hematite solid solution series with special reference to the phenomenon of reverse thermoremanent magnetism, Ph. D. Dissertation, Princeton of rocks under the effect of mechanical stresses, *Tectonophys., 9*, 167-195, 1970.
83. Nagata, T., and H. Kinoshita, Effect of hydrostatic pressure on magnetostriction and magnetocrystalline anisotropy of magnetite, *Phys. Earth Planet. Inter., 1*, 44-48, 1967.
84. Nininger, R. C., Jr., and D. Schroeer, Mössbauer studies of the Morin transition in bulk and microcrystalline α-Fe_2O_3, *J. Phys. Chem. Solids, 39*, 137-144, 1978.
85. Nishitani, T., and M. Kono, Curie temperature and lattice constant of oxidized titanomagnetite, *Geophys. J. R. Astr. Soc., 74*, 585-600, 1983.
86. Nishitani, T., and M. Kono, Effect of low-temperature oxidation on the remanence properties of titanomagnetites, *J. Geomag. Geoelectr., 41*, 19-38, 1989.
87. O'Donovan, J. B., D. Facey, and W. O'Reilly, The magnetization process in titanomagnetite ($Fe_{2.4}Ti_{0.6}O_4$) in the 1–30 μm particle size range, *Geophys. J. R. Astr. Soc., 87*, 897-916, 1986.
88. O'Reilly, W., *Rock and Mineral Magnetism*, 230 pp., Blackie, Glasgow, 1984.
89. Özdemir, Ö., An experimental study of thermoremanent magnetization acquired by synthetic monodomain titanomagnetites and titnomaghemites, Ph. D. Dissertation, University of Newcastle upon Tyne, 1979.
90. Özdemir, Ö., and S. K. Banerjee, A preliminary magnetic study of soil samples from west-central Minnesota, *Earth Planet. Sci. Lett., 59*, 393-403, 1982.
91. Özdemir, Ö., and D. J. Dunlop, Crystallization remanent magnetization during the transformation of maghemite to hematite, *J. Geophys. Res., 93B*, 6530-6544, 1988.
92. Özdemir, Ö., and D. J. Dunlop, Chemico-viscous remanent magnetization in the Fe_3O_4–γFe_2O_3 system, *Science, 243*, 1043-1047, 1989.
93. Özdemir, Ö., and W. O'Reilly, An experimental study of thermoremanent magnetization acquired by synthetic monodomain titanomaghemites, *J. Geomag. Geoelectr., 34*, 467-478, 1983.
94. Ozima, M., and E. E. Larson, Low- and high-temperature oxidation of titanomagnetite in relation to irreversible changes in the magnetic properties of submarine basalts, *J. Geophys. Res., 75*, 1003-1018, 1970.
95. Parasnis, D. S., *Principles of Applied Geophysics*, 3rd ed., 275 pp., Chapman and Hall, London, 1979.
96. Pauthenet, R., Variation thermique de l'aimantation spontaneé des ferrites de nickel, cobalt, fer et manganèse, *C. R. Acad. Sci. (Paris), Sér. B, 230*, 1842-1844, 1950.
97. Pick, T., and L. Tauxe, Chemical remanent magnetization in synthetic Fe_3O_4, *J. Geophys. Res., 96B*, 9925-9936, 1991.
98. Radhakrishnamurty, C., and E. R. Deutsch, Magnetic techniques for ascertaining the nature of iron oxide grains in basalts, *J. Geophys., 40*, 453-465, 1974.
99. Radhakrishnamurty, C., S. D. Likhite, E. R. Deutsch, and G. S. Murthy, A comparison of the magnetic properties of synthetic titanomagnetites and basalts, *Phys. Earth Planet. Inter., 26*, 37-46, 1981.
100. Robins, B. W., Remanent magnetization in spinel iron-oxides, Ph. D. Dissertation, University of New South Wales, 1972.
101. Rochette, P., et al., Magnetic transition at 30-34 Kelvin in pyrrhotite: insight into a widespread occurrence of this mineral in rocks, *Earth Planet. Sci. Lett., 98*, 319-328, 1990.
102. Roquet, J., Sur les rémanences magnétiques des oxydes de fer et leur intérêt en géomagnétisme, *Ann. Géophys., 10*, 226-247 and 282-325, 1954.
103. Schmidbauer, E., and P. W. Readman, Low temperature magnetic properties of Ti-rich Fe-Ti spinels, *J. Magn. Magn. Mater., 27*, 114-118, 1982.
104. Schmidbauer, E., and N. Schembera, Magnetic hysteresis properties and anhysteretic remanent magnetization of spherical Fe_3O_4 particles in the grain size range 60–160 nm, *Phys. Earth Planet. Inter., 46*, 77-83, 1987.
105. Schult, A., Effect of pressure of the

Curie temperature of titanomagnetites [(1-x)·Fe_3O_4–x·$TiFe_2O_4$], *Earth Planet. Sci. Lett.*, *10*, 81-86, 1970.

106. Senftle, F. E., A. N. Thorpe, C. Briggs, C. Alexander, J. Minkin, and D. L. Griscom, The Néel transition and magnetic properties of terrestrial, synthetic, and lunar ilmenites, *Earth Planet. Sci. Lett.*, *26*, 377-386, 1975.
107. Sharma, P. V., *Geophysical Methods in Geology*, 2nd ed., 442 pp., Elsevier, New York, 1986.
108. Shirane, G., D. E. Cox, W. J. Takei, and S. L. Ruby, A study of the magnetic properties of the $FeTiO_3$–αFe_2TiO_3 system by neutron diffraction and the Mössbauer effect, *J. Phys. Soc. Jpn.*, *17*, 1598-1611, 1962.
109. Shive, P. N., and D. M. Fountain, Magnetic mineralogy in an Archean crustal section: implications for crustal magnetization, *J. Geophys. Res.*, *93B*, 12,177-12,186, 1988.
110. Soffel, H. C., Pseudo-single domain effects and the single domain-multidomain transition in natural pyrrhotite deduced from domain structure observations, *J. Geophys.*, *42*, 351-359, 1977.
111. Stacey, F. D., and S. K. Banerjee, *The Physical Principles of Rock Magnetism*, 195 pp., Elsevier, Amsterdam, 1974.
112. Stokking, L. B., and L. Tauxe, Acquisition of chemical remanent magnetization by synthetic iron oxide, *Nature*, *327*, 610-612, 1987.
113. Syono, Y., Magnetocrystalline anisotropy and magnetostriction of Fe_3O_4–Fe_2TiO_4 series, with special application to rock magnetism, *Jpn. J. Geophys.*, *4*, 71-143, 1965.
114. Telford, W. M., L. P. Geldart, and R. E. Sheriff, *Applied Geophysics*, 2nd ed., 770 pp., Cambridge University Press, New York, 1990.
115. Thompson, R., and F. Oldfield (Eds.), *Environmental Magnetism*, 227 pp., Allen and Unwin, London, 1986.
116. Toft, P. B., and J. Arkani-Hamed, Magnetization of the Pacific Ocean lithosphere deduced from MAGSAT data, *J. Geophys. Res.*, *97B*, 4387-4406, 1992.
117. Tucker, P., Low-temperature magnetic hysteresis properties of multidomain single-crystal titanomagnetite, *Earth Planet. Sci. Lett.*, *54*, 167-172, 1981.
118. Tucker, P., and W. O'Reilly, A magnetic study of single crystal titanomagnetite ($Fe_{2.4}Ti_{0.6}O_4$), *Phys. Earth Planet. Inter.*, *16*, 183-189, 1978.
119. Tucker, P., and W. O'Reilly, The acquisition of thermoremanent magnetization by multidomain single crystal titanomagnetite, *Geophys. J. R. Astr. Soc.*, *60*, 21-36, 1980.
120. Uyeda, S., Thermo-remanent magnetism as a medium of palaeomagnetism, with special reference to reverse thermo-remanent magnetism, *Jpn. J. Geophys.*, 2, 1-123, 1958.
121. von Philipsborn, H., and L. Treitinger, Spinels, in *Landolt-Börnstein Numerical Data and Functional Relationships in Science and Technology; Group III: Crystal and Solid State Physics; vol. 12b, Magnetic and Other Properties of Oxides and Related Compounds*, edited by K.-H. Hellwege and A. M. Hellwege, pp. 54-284, Springer-Verlag, New York, 1980.
122. Wasilewski, P. J., and M. A. Mayhew, Crustal xenolith magnetic properties and long wavelength anomaly source requirements, *Geophys. Res. Lett.*, *9*, 329-332, 1982.
123. Wasilewski, P. J., and M. A. Mayhew, The Moho as a magnetic boundary revisited, *Geophys. Res. Lett.*, *19*, 2259-2262, 1992.
124. Wechsler, B., D. H. Lindsley, and C. T. Prewitt, Crystal structure and cation distribution in titanomagnetites ($Fe_{3-x}Ti_xO_4$), *Am. Mineral.*, *69*, 754-770, 1984.
125. Westcott-Lewis, M. F., and L. G. Parry, Magnetism in rhombohedral iron-titanium oxides, *Aust. J. Phys.*, *24*, 719-734, 1971.
126. Williams, M. C., P. N. Shive, D. M. Fountain, and R. B. Frost., Magnetic properties of exposed deep crustal rocks from the Superior Province of Manitoba, *Earth Planet. Sci. Lett.*, *76*, 176-184, 1985/86.
127. Worm, H.-U., Multidomain susceptibility and anomalously strong low field dependence of induced magnetization in pyrrhotite, *Phys. Earth Planet. Inter.*, *69*, 112-118, 1991.
128. Worm, H.-U., and H. Markert, Magnetic hysteresis properties of fine particle titanomagnetites precipitated in a silicate matrix, *Phys. Earth Planet. Inter.*, *46*, 84-93, 1987.